http://dx.doi.org/10.5012/bkcs.2012.33.1.149

3D-QSAR Study of Melanin Inhibiting (*S*)-(+)-Decursin and its Analogues by Pharmacophore Mapping

Kyeong Lee,[a] Sang Won Jung,[†,a] Ravi Naik, and Art E. Cho[†,*]

College of pharmacy, Dongguk University-Seoul, Seoul 100-715, Korea
[†]Department of Bioinformatics, Korea University, Yeongi-gun, Chungnam 339-700, Korea. [*]E-mail: artcho@korea.ac.kr
Received September 30, 2011, Accepted November 15, 2011

The (*S*)-(+)-decursin and its analogues are reported as potent inhibitors of melanin production in B16 murine melanoma cells. In order to understand the factors responsible for potency as well as inhibition of potency of (*S*)-(+)-decursin and its analogues, three-dimensional quantitative structure-activity relationship (3D-QSAR) studies were performed. Since receptor structures are not available, a pharmacophore model was constructed. Using PHASE, we generated 3 different models and selected the seven-site model, which returned excellent statistical values (r^2 = 0.9127, Q^2 = 0.6878, Pearson-R = 0.9014). Using the generated pharmacophore model, we screened a natural products library and obtained 4'-*epi*-decursin as the most related compound. 4'-*epi*-decursin is similar to (*S*)-(+)-decursin, but shows additional interaction possibilities with tyrosinase. The study thus sheds some light on possibility of developing more potent tyrosinase inhibitors.

Key Words : Pharmacophore, (*S*)-(+)-Decursin, Melanin inhibitors, 3D-QSAR, PHASE

Introduction

Melanosomes are intracellular membrane-bound organelles within which melanin's are synthesized and stored in specialized pigment cells, including melanocytes and retinal and iris pigment epithelial cells.[1] Melanin plays a very important role in protecting human skin from the noxious effects of sunlight, toxic drugs and various chemicals.[2] However, hyper-pigmentation of the skin is a common problem that is prevalent in middle aged and elderly people. It is caused by over production of melanin inside the body. Tyrosine enzyme is known to be the key enzyme in melanin production.[3,19] Increased levels of melanin production known to cause diverse hyper-pigmentary disorders such as melasma, freckles, age sports and actinic damage, which result in the accumulation of increased levels of epidermal and dermal pigmentation. Thus therapeutic means for the treatment of dermatological disorders and the development of cosmetic whitening agent can be achieved by means of inhibition of abnormal deposition of melanin.[2,4-6]

The (*S*)-(+)-decursin and its analogues are novel candidates for cancer treatment as well, which are isolated from Angelica gigasNakai plant and were known to exhibit wide range of biological properties. We reported that these analogues were found to be potent inhibitors of melanin production in B16 melanoma cells. In order to understand the factors affecting the activity of (*S*)-(+)-decursin as potent inhibitor of melanin production, three-dimensional-quantitative structure-activity relationship (3D-QSAR) studies were performed. 3D-QSAR methods have been developed to visually examine the steric and electrostatic fields surrounding binding sites. It requires three-dimensional structures to calculate energies. For this purpose, we used PHASE program of Schrödinger suite to generate pharmacophore models.[2,7]

Materials and Methods

Data Sets. A set of 33, (*S*)-(+)-decursin and its analogues as potent inhibitors of melanin formation, from our previously published work, was used for pharmacophore generation. In the previous work, the biological activities of these compounds were measured as inhibition rate at 100 μM and we converted these values to IC_{50} assuming linear relation around the data points.[2] It is a reasonable assumption given that most of the measured inhibition rates hover about 50%. These converted values, along with their negative logarithms that were eventually used in our 3D-QSAR study, are tabulated in Table 1.

Preparation of Ligands. Structures of the compounds were generated by 2D sketcher and LigPrep module of Schrödinger.[14] Conformers for each ligand were generated using Mixed MCMM/LMOD method with OPLS-2005 force field and implicit distance-dependent dielectric solvent model at cutoff root mean square deviation (RMSD) of 1 Å. For each molecule, conformers with the maximum energy difference of 30 kcal/mol relative to the global energy minimum conformer were obtained.

Generation of Common Pharmacophore Hypothesis. Common pharmacophore hypothesis (CPH) was generated using PHASE from Schrödinger.[16,17] Pharmacophore features - hydrogen bond acceptor (A), hydrogen bond donor (D), hydrophobic group (H), and aromatic ring (R) - were defined by a set of chemical structure patterns by PHASE. PHASE assigns features one of the three possible geometries - point, vector, or group - which define physical characteristic of the

[a]These authors contributed equally to this work.

site using SMARTS queries. Common pharmacophores were then identified from set of variants using tree-based partition algorithm with the maximum tree depth of 5. The final size of pharmacophore box, which governs the tolerance on matching, was 2 Å. Any pharmacophore in the group could ultimately become a CPH. These CPHs were examined using a scoring function to yield the best alignment of the active ligands.[7,8]

Pharmacophore Screening. Common pharmacophore model was used to search for new inhibitors. Natural products (73,421 molecules) from ZINC chemical database were screened to find matches to our hypothesis.[18] Conformers were generated during search using ConfGen module.[15] We imposed the condition that all molecules must match on at least 7 site points with distance matching tolerance 1.0 Å, with other parameters in default setting.

Results and Discussion

Pharmacophore Model Development and Validation. Pharmacophore models containing five, six, and seven sites were generated using a terminal box size of 1 Å with 4 active molecules, belonging to (*S*)-(+)-decursin and its derivatives and selected using a tree based partition algorithm. The test set molecules were so selected as to cover a wide distribution of potencies, otherwise randomly. In Table 1, the last column indicates which compounds belong to the test set. The five- and six-featured CPHs were rejected, as they were unable to define the complete binding space of the selected molecules. A total of 186 seven-featured CPHs

Table 1. Melanin inhibitory activity and cytotoxicity of compounds **1-8** and **13** in B16F10 murine melanoma cells

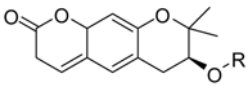

Compound	R	IC_{50} (μM)	pIC_{50}	Training set/test set
1	-H	410	3.39	Test set
2	-COCH=C(CH_3)$_2$	70	4.15	Training set
3	-COcis-C(CH_3)=CHCH_3	67	4.17	Training set
4a	-COtrans-C(CH_3)=CHCH_3	70	4.15	Training set
4b	-COC(CH_3)=CH_2	86	4.07	Training set
4c	-COCH=CHCH_2CH_3	63	4.20	Training set
4d	-COCH_2CH=CH_2	5000	2.30	Training set
4e	-COCH_2CH_2CH=CH_2	137	3.86	Training set
5a	-COCH_3	5000	2.30	Training set
5b	-CO(CH_2)$_3CH_3$	65	4.19	Training set
5c	-CO(CH_2)$_8CH_3$	63	4.20	Training set
6a	-COCH=CH-3-Pyridyl	93	4.03	Training set
6b	-COCH=CH-2-Thienyl	70	4.15	Test set
6c	-COCH=CH-2-Furanyl	152	3.82	Test set
7a	-COCH=CH-Phenyl	69	4.16	Training set
7b	-COCH=CH-C_6H_4-OCH_3-2	78	4.11	Training set
7c	-COCH=CH-C_6H_4-OH-2	65	4.19	Test set
7d	-COCH=CH-C_6H_4-OAc-2	76	4.12	Training set
7e	-COCH=CH-C_6H_4-OCH_3-3	132	3.88	Training set
7f	-COCH=CH-C_6H_4-OH-3	68	4.17	Training set
7g	-COCH=CH-C_6H_4-OAc-3	62	4.21	Training set
7h	-COCH=CH-C_6H_4-OCH_3-4	124	3.91	Test set
7i	-COCH=CH-C_6H_4-OH-4	75	4..12	Training set
7j	-COCH=CH-C_6H_4-OAc-4	66	4.18	Training set
7k	-COCH=CH-C_6H_3-(OCH_3)$_2$-3,4	118	3.93	Training set
7l	-COCH=CH-C_6H_3-(OH)$_2$-3,4	115	3.94	Test set
7m	-COCH=CH-C_6H_3-(OAc)$_2$-3,4	163	3.79	Training set
7n	-COCH=CH-C_6H_2-(OCH_3)$_3$-3,4,5	266	3.58	Training set
7o	-COCH=CH-C_6H_2-(OH)$_3$-3,4,5	84	4.08	Training set
7p	-COCH=CH-C_6H_2-(OAc)$_3$-3,4,5	141	3.85	Training set
8a	-COCH_2CH_2-Phenyl	80	4.10	Training set
8b	-COCH_2CH_2-C_6H_4-OCH_3-2	73	4.14	Training set
13	-CH_2CH=CH-Phenyl	148	3.93	Training set
Arbutin	Reference	610	3.21	Training set

Table 2. Summary of PLS analysis results for five best CPHs. SD, standard deviation of the regression; r^2, value of r^2 for the regression; F, variance ratio; P, significance level of variance ratio; RMSE, root-mean-square error; Q^2, value of Q^2 for the predicted activities; Pearson-R, correlation between the predicted and observed activity for the test set

Pharma-cophore	CPH1	CPH2	CPH3	CPH4	CPH5
SD	0.1161	0.1174	0.1236	0.1475	0.1614
r^2	0.9127	0.9107	0.901	0.859	0.8312
F	240.4	234.4	209.4	140.1	113.3
P	1.14E-13	1.49E-13	4.85E-13	2.91E-11	2.33E-10
RMSE	0.1469	0.1705	0.1445	0.1778	0.1896
Q^2	0.6878	0.5796	0.6981	0.563	0.4802
Pearson-R	0.9014	0.8759	0.8948	0.8887	0.8959

belonging to 6 types (AAAAHHR, AAAHHRR, AAHHHRR, AAAAHHH, AAAHHHR, and AAAAHRR) were subjected to scoring function analysis with respect to actives using default parameters for site, vector, and volume. Reference ligand activity was included in the score with a weight of 3.21 from compound arbutin[9]. The hypotheses that survived the scoring process were used to build an atom-based QSAR model. A summary of statistical data of the best CPHs, labeled CPH1 to CPH5, with their results are listed in Table 2.

CPH1 for each combination displayed consistent and satisfactory external predictivity as compared to the others. CPH1 showed a good r^2 value for the training set (0.9127) and excellent predictive power with q^2 of 0.6878. A good Pearson-R value of 0.9015 was also observed. Hence, the hypothesis CPH1 with four hydrogen bond acceptors (A), one hydrophobic group (H), and two aromatic rings (R) as pharmacophoric features was retained for further studies. Figure 1 shows the alignment of the molecules under study along with CPH1. Figure 2 shows the graph of actual vs. predicted activity for training and test set molecules.[7,8] It should be noted that there are 2 compounds belonging to the

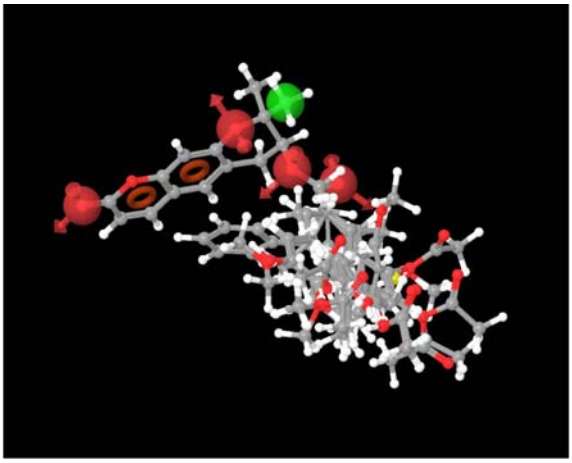

Figure 1. Common pharmacophore hypothesis **1** (CPH1) based alignment of (+)-decursin and its derivatives.

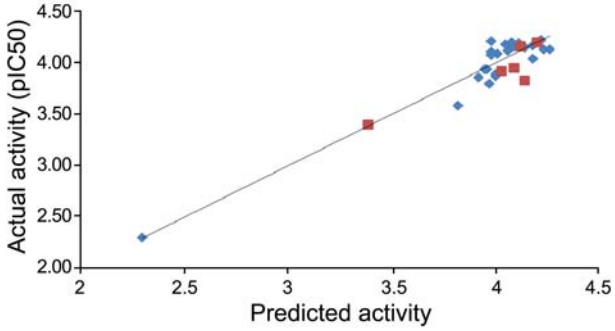

Figure 2. Scatter plot of actual activity versus PHASE predicted activity (Blue: training set; Red: test set).

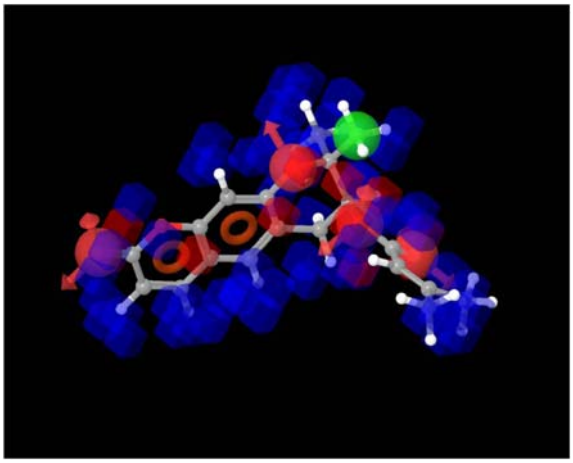

Figure 3. PHASE 3D-QSAR plot displayed for CPH1. Blue cube is for positive coefficient, which indicates the increase in activity; and red cube is for negative coefficient, which indicates the decrease in activity.

training set with pIC value of 2.3 and their existence greatly enhanced r^2 value. Without these compounds, r^2 value turns out to be 0.5062. This shows that spread of activity in training sets is important.

Interpretation of QSAR Models. The QSAR results can best be visualized using 3D plots of crucial pharmacophore regions as in Figure 3. The cubes that represent the model are colored according to the sign of their coefficient values. Blue cubes refer to positive coefficients, which correspond to increase in activity, whereas red cubes refer to negative coefficients indicating the same ligand feature substitution with decrease in activity. Carbonyl part of compound can interact with copper ion in tyrosinase as a hydrogen bond acceptor, and two aromatic rings might have a hydrophobic or π-π interaction with histidine residue or hydrophobic residue in active site. Ester group plays a key factor in forming hydrogen bond with one of residues of tyrosinase. Additional substitution of this group can help discover more potent inhibitors.[10,11]

Pharmacophore Model Screening Results. Through the pharmacophore screening, 17 compounds were found and finally the most related compound ZINC08917974 was selected (Fig. 4). It is known as 4'-*epi*-decursin,[13] one of Angelica gigasNakai extracts like (*S*)-(+)-decursin. There

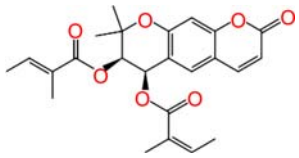

Figure 4. Chemical structure of natural compound (ZINC 08917974).

has been a report that this compound has anti-inflammatory potential.[12] From our analysis using the pharmacophore model, 4'-*epi*-decursin and its analogues can have additional interactions with tyrosinase and hence can be a platform for design of more potent inhibitors.

Conclusions

In this work, we have constructed a pharmacophore model for tyrosinase inhibitors with experimentally verified (*S*)-(+)-decursin and its analogues using PHASE from Schrödinger suite. The best hypothesis consisted of seven pharmacophoric features. It exhibited good r^2 (0.9127), q^2 (0.6878), and Pearson-R (0.9015) values. With this model, we performed pharmacophore screening on a natural products library and selected 4'-*epi*-decursin, which is similar to (S)-(+)-decursin. In fact, 4'-*epi*-decursin possesses additional interactions on top of all the interactions (*S*)-(+)-decursin shows. This means that further development along this line can yield more potent inhibitors of tyrosinase. Since there is no experimentally solved structure of human form of tyrosinase, it is not feasible to perform receptor based 3D-QSAR analysis or docking. However, it would be interesting see how docking to homology model of tyrosinase would compare to pharmacophore models. Currently, this line of work is being pursued in our laboratory.

Acknowledgments. This work was supported by the Dongguk University Research Fund of 2010, Republic of Korea (KL and RN).

References

1. Watt, B.; Rapaso, G.; Mark, M. S. *Func. Amyloid Aggregation* **2010**, 89-113.
2. Lee, K.; Lee, J. H.; Boovanahalli, S. K.; Choi, Y.; Choo, S.-J.; Yoo, I.-D.; Kim, D. H.; Yun, M. Y.; Lee, G. W.; Song, G. Y. *Eur. J. Med. Chem.* **2010**, *45*, 5567-5575.
3. Mapunya, M. B.; Hussein, A. A.; Rodriguez, B.; Lall, N. *Phytomedicine* **2011**, *18*(11), 1006-1012.
4. Lee, N. K.; Son, K. H.; Chang, H. W.; Kang, S. S.; Park, H.; Heo, M. Y.; Kim, H. P. *Arch. Pharm. Res.* **2004**, *27*, 1132-1135.
5. Solano, F.; Briganti, S.; Picardo, M.; Ghanem, G. *Pigment Cell. Res.* **2006**, 550-571.
6. Curto, E. V.; Kwong, C.; Hermersdorfer, H.; Glatt, H.; Santis, C.; Virador, V.; Hearing, V. J.; Dooley, T. P. *Biochem. Pharmacol.* **1999**, *57*, 663-672.
7. Chung, J. Y.; Pasha, F. A.; Cho, S. J.; Won, M.; Lee, J. J.; Lee, K. *Arch. Pharm. Res.* **2009**, *32*(3), 317-323.
8. Gadhe, C. G.; Madhavan, G.; Kothandan, G.; Lee, T. B.; Lee, K.; Cho, S. J. *Bull. Korean Chem. Soc.* **2011**, *32*(5), 1-7.
9. Kubo, I.; Nihei, K.; Tsujimoto, K. *Bioorg. Med. Chem.* **2004**, *12*, 5349-5354.
10. Wei, Y.; Carole, D.; Samir, Y.; Ramain, H.; Catherine, B.; Huacan, S.; Renaud, H.; Marius, R.; Ahcène, B. *Eur. J. Med. Chem.* **2011**, *46*, 4330-4335.
11. Okombi, S.; Rival, D.; Bonnet, S.; Mariotte, A. M.; Perrier, E.; Boumendjel, A. *Bioorg. Med. Chem. Lett.* **2006**, *16*, 2252-2255.
12. Kummala, T.; Vuorela, P.; Johansson, S.; Bohlin, L.; Vuorela, H.; Vasange, M. *Pharmaceut. Pharmacol. Lett.* **1998**, *8*, 144-147.
13. Sano, K.; Yosioka, I.; Kitawa, I. *Chem. Pharm. Bull.* **1975**, *23*, 20-28.
14. LigPrep, version 2.5, Schrödinger, LLC, New York, NY, 2011.
15. Watts, K. S.; Dalai, P.; Murphy, R. B.; Sherman, W.; Friesner, R. A.; Shelley, J. C. *J. Chem. Inf. Model.* **2010**, *50*, 534-546.
16. Dixon, S. L.; Smondyrev, A. M.; Knoll, E. H.; Shaw, D. E.; Friesner, R. A. *J. Comput. Aided Mol. Des.* **2006**, *20*, 647-671.
17. Dixon, S. L.; Smondyrev, A. M.; Rao, S. N. *Chem. Biol. Drug. Des.* **2006**, *67*, 370-372.
18. Irwin, J. J.; Schoichet, B. K. *J. Chem. Inf. Model.* **2005**, *45*, 177-182.
19. Matoba, M.; Kumagi, T.; Yamamoto, A.; Yoshitsu, H.; Sugiyama, M. *J. Biol. Chem.* **2006**, *281*, 8981-8990.